

See discussions, stats, and author profiles for this publication at: <https://www.researchgate.net/publication/339634416>

Seasonal Risk Assessment of Water–Electricity Nexus Systems under Water Consumption Policy Constraint

Article in *Environmental Science and Technology* · March 2020

DOI: 10.1021/acs.est.0c00171

CITATIONS

3

READS

97

4 authors, including:



Mengfei Mu

Chinese Academy of Sciences

6 PUBLICATIONS 33 CITATIONS

[SEE PROFILE](#)



Zhenxing Zhang

University of Illinois, Urbana-Champaign

66 PUBLICATIONS 1,460 CITATIONS

[SEE PROFILE](#)

Seasonal Risk Assessment of Water–Electricity Nexus Systems under Water Consumption Policy Constraint

Mengfei Mu, Zhenxing Zhang,* Ximing Cai, and Qihong Tang*



Cite This: *Environ. Sci. Technol.* 2020, 54, 3793–3802



Read Online

ACCESS |



Metrics & More



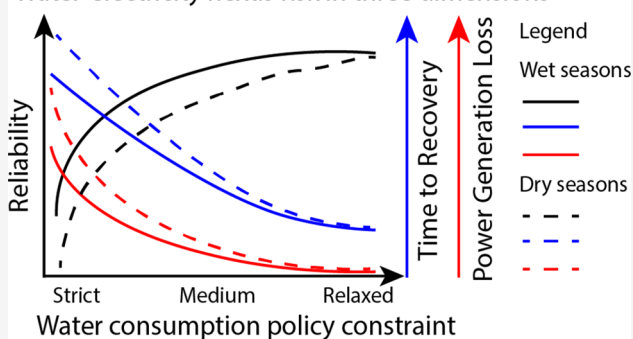
Article Recommendations



Supporting Information

ABSTRACT: Previous studies have estimated power plant cooling water consumption based on the long-term average cooling water consumption intensity (WI: water consumption per unit of electricity generation) at an annual scale. However, the impacts of the seasonality of WI and streamflow on electricity generation are less well understood. In this study, a risk assessment method is developed to explore the seasonal risk of water–electricity nexus based on the Integrated Environmental Control Model, which can simulate variable WIs in response to daily weather conditions and avoid underestimation in WIs as well as nexus risk during dry seasons. Three indicators, reliability, maximum time to recovery, and total power generation loss, are proposed to quantify the seasonal nexus risk under water consumption policy constraint represented by the allowed maximum percentage of water consumption to streamflow. The applications of the method in two representative watersheds demonstrate that the nexus risk is highly seasonal and is greatly impacted by the seasonal variability of streamflow rather than annual average water resources conditions on which most previous studies are based. The nexus is found more risky in the watershed with almost double mean annual streamflow and greater streamflow variability, compared with the watershed with less streamflow variability.

Water–electricity nexus risk in three dimensions



1. INTRODUCTION

A significant amount of water is consumed in the cooling processes of electricity generation in thermal power plants all over the world.¹ Trade-offs between water and energy for now and in the future have been investigated in the United States,^{2–5} China,^{6–8} and other regions,^{9–14} mainly focusing on annual-scale estimates^{15–17} or long-term projected trends.^{18,19} Seasonal variabilities of cooling water consumption (WC) and the associated water–electricity nexus risk have recently attracted attention. For example, seasonal variabilities of cooling water consumption intensity (WI) are revealed based on field data;²⁰ seasonal aspects of water–hydropower nexus are explored²¹ while there is still a lack of knowledge on the seasonality of the water–thermoelectricity nexus, which is the focus of our study. Cooling water consumption usually has a minimal impact on streamflow and the water resources system in wet seasons or at annual to decadal scales.²² However, the incidence of high cooling water consumption, high water demand from other users, and low water availability in dry seasons or drought events may put both electricity generation and the water supply at great risk,²³ which we refer to as the water–electricity nexus risk. On the one hand, low cooling water availability limits the contribution of plants to the power grid when a large amount of electricity is demanded. On the other hand, high cooling water consumption by plants competes with other water uses and exerts pressure on the

water supply to other consumers when water demand increases during dry seasons. These risks may be greatly underestimated if the assessment is conducted at an annual scale. Therefore, a seasonal-scale assessment is more critically required to identify the potential nexus risk and its timing.

Most studies base cooling water consumption estimates on an average cooling water consumption intensity^{24–27} throughout the assessment period according to power plant design characteristics, such as fuel type, cooling system type, and combustion technology. This would also lead to further underestimates in dry-season WI,²⁰ WC, and the associated risk. A power plant operation modeling tool called the Integrated Environmental Control Model (IECM)^{28–30} shows the potential to simulate variable WIs over periods by considering the temporal variability of ambient climate conditions³¹ in addition to plant characteristics.

The objectives of this study are 2-fold. First, we contribute a quantitative risk assessment method to evaluate the seasonal

Received: January 9, 2020
 Revised: February 26, 2020
 Accepted: March 2, 2020
 Published: March 2, 2020



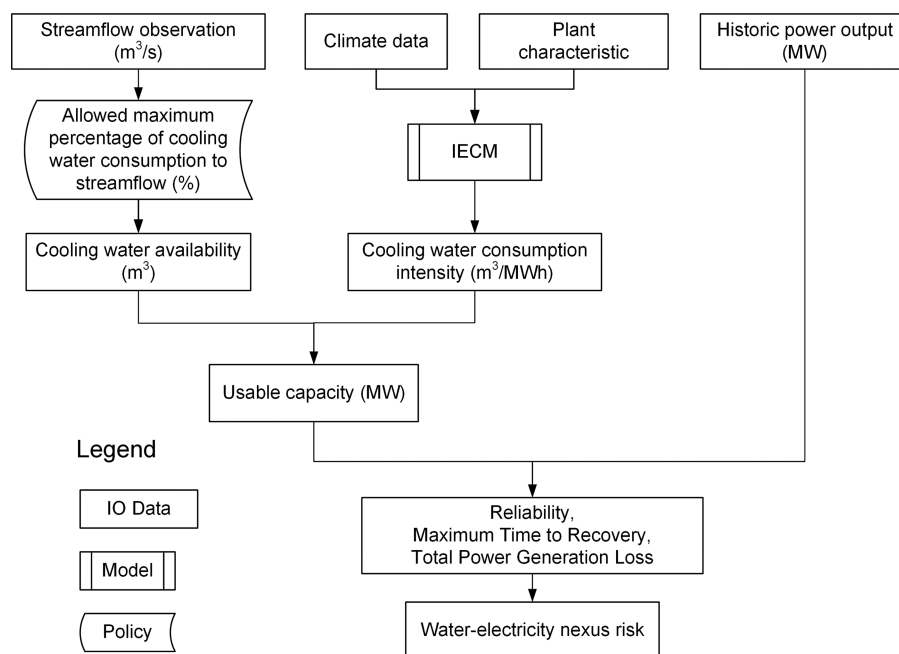


Figure 1. Workflow of the water–electricity nexus risk assessment method at a power plant level.

risk of the water–electricity nexus at the power plant level under a water consumption policy constraint in terms of the allowed maximum percentage^{12,19,32,33} of cooling water consumption to streamflow. This method considers daily variations of WI, electricity generation, and streamflow. Three indicators, including reliability, maximum time to recovery, and total power generation loss,^{34,35} are defined to quantify the risk in different seasons. Second, the proposed method is tested and applied to two representative watersheds, the Kaskaskia River watershed in the U.S. Midwest and the San Juan River watershed in the Southwest. The seasonal risk of the water–electricity nexus at a plant level under varying water consumption policy constraints is investigated and compared in these two watersheds. Implications can be provided to policymakers to balance the trade-off between water resources reservation and electricity generation. We highlight the necessity and advantages of a seasonal-scale assessment over that of an annual scale in future electricity capacity expansion planning as well as in water consumption policy design and practice.

2. MATERIALS AND METHODS

2.1. The Risk Assessment Method. The workflow of the proposed risk assessment method is presented in Figure 1. First, the cooling water availability based on daily streamflow³⁶ is calculated under a water consumption policy constraint in terms of the allowed maximum percentage of daily cooling water consumption to streamflow, which has been adopted in previous studies^{12,19,32,33} and by a water resources agency³⁷ to constrain cooling water consumption. Second, climate data, such as air temperature and relative humidity, retrieved from the North American Land Data Assimilation System Project Phase Two (NLDAS-2) database^{38,39} and power plant characteristics data from the Energy Information Administration Form 860 (EIA-860) database⁴⁰ are taken as inputs to the IECM modeling tool to simulate the daily WI. Third, the daily usable capacity of electricity generation by a power plant is estimated based on cooling water availability and the WI.

Finally, the time series of daily usable capacity is compared with the historic level of power generation output to calculate the three quantitative indicators, reliability, maximum time to recovery, and total power generation loss, to reveal the water–electricity nexus risk at the seasonal scale. The IECM and the calculation of variable WIs are introduced in Section 2.2. Definitions of the three quantitative indicators are described in Section 2.3. The detailed description of the input data used in the assessment is provided in Supporting Information (SI) Section S-1.

2.2. Integrated Environmental Control Model. The Integrated Environmental Control Model (IECM Version 11.2)^{28–30} is a publicly available modeling tool developed by Carnegie Mellon University to simulate the plant operation, including the cooling performance of individual thermal power plants. The water system module embedded in the IECM estimates cooling water consumption at power plants based on mass and energy balances with the inputs such as fuel type, cooling technology, and ambient climate conditions. IECM has been used extensively in previous studies^{29,31,41,42,43} to estimate the water use at various stages of the entire fuel life cycle. In this study, we focus on the plant operation stage involving cooling water consumption that usually accounts for more than 90%⁴³ of the total life-cycle water consumption.

One of the advantages of the IECM is its capability to consider the impacts of ambient climate conditions, that is, air temperature and relative humidity,³¹ on the performance of the wet cooling tower and the associated WI. WI is projected to increase by 5% ~ 10% by the end of this century because of climate change.³¹ However, the seasonal variability of the climate conditions⁴⁴ is usually much larger than the interannual or climate-change-induced variability but has not been considered in previous studies. The large temporal variability in ambient climate conditions may lead to the significant seasonality of the WI. (The intake water temperature is not taken into account in the IECM or in this study as its impact on cooling performance of a wet-cooling-tower plant is usually minimal.⁴⁵ It should be noted that water temperature

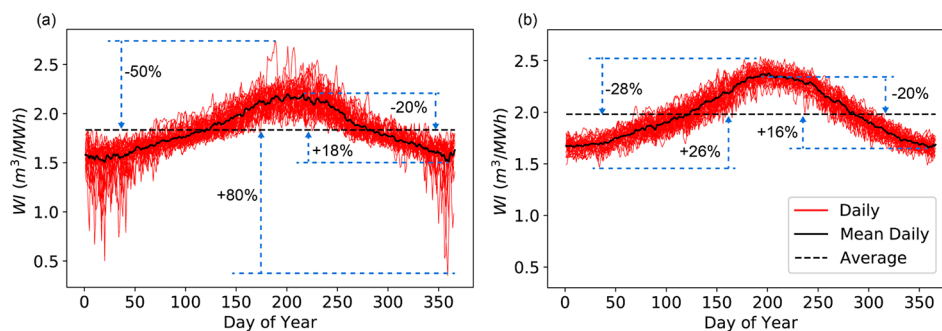


Figure 2. Daily cooling water consumption intensity (WI) during 1982–2012 (red line), mean daily WI (black solid line), and the average of daily WI (black dashed line) at the coal-fired power plant in (a) Kaskaskia River watershed and (b) San Juan River watershed. The percentage values in the figure represent overestimates (positive values) or underestimates (negative values) of WI if using the average WI as in previous studies rather than the daily or mean daily WI.

plays an important role and should be taken into account for a once-through power plant.) Most of the cooling water is consumed by evaporation at a wet-cooling-tower plant. The daily cooling water consumption intensity can be expressed as a function of daily air temperature and relative humidity (refer to SI Section S-3 and IECM documentation for detailed calculation of WI):

$$WI_t = f(T_t^{\text{air}}, RH_t) \quad (1)$$

where t is the daily time index, T_t^{air} is the daily average air temperature ($^{\circ}\text{C}$). RH_t is the relative humidity (%), calculated as the following:^{46,47}

$$RH_t = 0.263p_t q_t \times \exp\left[\frac{17.67(T_t^{\text{air}} - T_0)}{T_t^{\text{air}} - 29.65}\right]^{-1} \quad (2)$$

where p_t is the air pressure (Pa), q_t is the specific humidity (kg/kg), T_0 is the triple point of water (273.16 K), and T_t^{air} is the air temperature (K).

A major obstacle to closely integrating the IECM with the proposed risk assessment method is that the IECM source codes are not released publicly; thus, daily scale integration would require running the IECM manually numerous times. Therefore, a sensitivity test is conducted by running the IECM to determine the dominant climate factor that affects the WI. A regressed relationship between the WI and that dominant factor is obtained and conveniently incorporated into the risk assessment method. The sensitivity test results in two case studies are shown in Figure S2 in SI Section S-4. SI Figure S2a,c shows that the WI increases by as much as 70% (74%) when T^{air} increases from the minimal to the maximal air temperature with a constant average relative humidity in Kaskaskia (San Juan) watershed. Similarly, SI Figure S2b,d shows that the WI increases by only 6% (10%) when the RH decreases from the maximal to the minimal relative humidity with a constant average air temperature. Although T^{air} and RH are interacted with each other, WI is simplified to be estimated using variable T^{air} and average RH as WI is remarkably less sensitive to RH than to T^{air} as shown in the sensitivity test (SI Figure S2). Considering the impact of variable T^{air} under average RH can well capture most of the variations of WI (as shown in SI Figure S2) with a large coefficient of determination. Using average RH instead of variable RH in the regression function may induce some uncertainties in WI but these uncertainties are minimal (the maximum uncertainties are around 6–10%). With this simplification, it can greatly

benefit the integration of the risk assessment method. Therefore, the eq 1 is simplified to

$$WI_t = f(T_t^{\text{air}}, RH_{\text{ave}}) \quad (3)$$

where RH_{ave} is the long-term average relative humidity outside a power plant. A cubic polynomial regression is further conducted on the IECM-modeled WI to obtain a single-variable function (red solid line in SI Figure S2a,c) that links T^{air} to the WI:

$$WI_t = a \times (T_t^{\text{air}})^3 + b \times (T_t^{\text{air}})^2 + c \times T_t^{\text{air}} + d \quad (4)$$

where a , b , c , and d are the regression coefficients, which are unique to a specific power plant according to its plant characteristics and local climate conditions. For example, the regression coefficients are 3.12×10^{-5} , -7.46×10^{-4} , 1.82×10^{-2} , and 1.59, respectively, at the tested power plant in the Kaskaskia River watershed with a coefficient of determination R^2 as 0.98. Hereafter, eq 4 is used instead of the original IECM to calculate the daily WI to avoid manually filling in the massive input data and running the IECM. Equation 4 serves as a connection that bridges the IECM to the proposed risk assessment method with reasonable simplification and satisfactory accuracy, allowing us to analyze the seasonality of the cooling performance at a finer temporal resolution compared with the previous IECM-based studies.

Figure 2 demonstrates that the IECM-based WI has large daily to seasonal variations and could be significantly underestimated around 20% ~ 50% in hot seasons and overestimated around 16% ~ 80% in cold seasons if a constant value (shown by the black dashed line) is used as in previous studies. This shows the importance to use the variable daily WIs to estimate cooling water consumption and the associated seasonal risk. See a detailed explanation of the necessity of using the variable daily WIs in SI Section S-5. The advantages of considering variable WIs are also demonstrated in Section 3.3.

2.3. Quantification of the Water–Electricity Nexus Risk. First, we introduce the concept of the cooling water consumption percentage (R_t) to represent the impacts of electricity generation on water resources under no water consumption policy constraints, which means that power plants have unconstrained access to cooling water to support the historic level of electricity generation. R_t is defined as the percentage of daily cooling water consumption without the water consumption policy constraint to daily streamflow:

$$R_t = \frac{WC_t}{Q_t \times 24 \times 3600} \times 100\% = \frac{WI_t \times E_t}{Q_t \times 24 \times 3600} \times 100\% \quad (5)$$

where WC_t is the daily cooling water consumption (m^3) without the water consumption policy constraint, WI_t is the daily cooling water consumption intensity (m^3/MWh) calculated based on eq 4, E_t is the historic records of daily electricity generation (MWh) obtained from the EIA database, and Q_t is the daily streamflow (m^3/s). When a water consumption policy constraint in terms of the allowed maximum percentage (R^0) of cooling water consumption to streamflow is set to limit R_p , the cooling water availability would decrease, and the usable capacity (UC_t) of a power plant may be reduced to a level below the historic electricity generation output ($P_t = E_t/24$). Under a specific R^0 , UC_t is calculated as

$$UC_t = \min\left(\frac{3600 * Q_t * R^0}{WI_t}, C\right) \quad (6)$$

where the unit of UC_t is MW, C is the installed capacity (MW) of a power plant. Electricity generation capacity at a power plant is at risk of not meeting demand during a potential electricity undersupply period when its UC_t is smaller than P_t under a water consumption policy constraint, which means the power plant cannot supply as much electricity to the power grid as expected. In other words, the power plant would require more than the allowed maximum cooling water, exerting more impact on the water systems, if the historic level of electricity generation is to be achieved, that is, when UC_t equals P_t .

Three quantitative indicators, reliability, maximum time to recovery, and total power generation loss, have been widely used^{48–50} in the water resources system and policy design since being introduced (as concepts of reliability, resilience, and vulnerability). In this study, these indicators are used and modified to describe three different dimensions of the water–electricity nexus risk, respectively: (1) the probability of a power plant not exceeding the water quotas and violating the water consumption policy constraint while maintaining a desired historic level of electricity supply; (2) the maximum duration of the electricity undersupply periods when the daily usable capacity is always smaller than the historic power output; and (3) the total electricity supply deficit between the water-constrained electricity supply and historic electricity generation during the potential undersupply periods. These indicators are calculated based on the energy index with water resources conditions and policies as constraints, since our study focuses more on the constraint of water on power generation. The similar indicators can be defined based on the water index when the impacts of power generation on water systems need to be emphasized.

Reliability (Rel) is calculated as the probability (frequency) of the case when daily usable capacity is not smaller than the historic power output:

$$Rel = \text{Prob}(UC_t \geq P_t) = \frac{N_{UC \geq P_t}}{N} \times 100\% \quad (7)$$

where N is the total number of days during the study period and $N_{UC \geq P_t}$ is the total number of days when UC_t is not smaller than P_t . Note that $(1 - Rel)$ describes how often an electricity undersupply case may occur at a power plant.

Maximum time to recovery (MaxT) is defined to describe the duration of the longest electricity undersupply period, when UC_t on any day is smaller than P_t :

$$\text{MaxT} = \max_i D(UC_t \leq P_t), t \in T_i \quad (8)$$

where D is the duration (days) of the i th undersupply period T_i .

The third indicator total power generation loss (TotL) (MWh) during the undersupply periods T is calculated as

$$\text{TotL} = \sum_t (E_t - UC_t \times 24), \text{ where } t \in T \text{ and } UC_t \times 24 < E_t \quad (9)$$

By calculating these three quantitative indicators for the whole period and four seasons (every 3 months) during the years 1982–2012, we describe the probability, duration, and significance of the water–electricity nexus risk and their seasonal variabilities.

3. RESULTS

The proposed risk assessment method is applied to two representative watersheds (SI Figure S1) located in the United States: the Kaskaskia River watershed in Illinois in the U.S. Midwest and the San Juan River watershed in the U.S. Southwest. The long-term mean streamflow at the two selected streamflow gage stations is $113 m^3/s$ with large seasonal variability and $52 m^3/s$ with small seasonal variability. A coal-fired power plant with a wet cooling tower and similar characteristics, such as a comparable maximum capacity, historic generation, and cooling water consumption is selected in each watershed. More details about the study areas can be found in SI Figure S1, Table S1, and Section S-2. The two watersheds host two similar power plants but with very different climate and streamflow conditions. Therefore, the comparative assessment shows the significant differences in the water–electricity nexus risk, as explained in the Results and Discussion sections.

3.1. Cooling Water Consumption Percentage under No Water Consumption Policy Constraint. This section shows the impacts of electricity generation on local streamflow when no water consumption policy is adopted to limit the cooling water availability. This represents the situation in which power plants can use as much cooling water as required to maintain their historic level of electricity generation.

Significant temporal variabilities exist in the mean monthly streamflow (Q), cooling water consumption (WC), and the percentage (R) of WC to Q , as shown in Figure 3. In the Kaskaskia River watershed (Figure 3a), there are adequate water resources in winter, but a very low streamflow in summer. The comparable peak WC occurs during June to September but with very different impacts on the water resources each month in terms of the R . The largest R occurs in September when the WC is high and the Q is the lowest. The R is smaller during June to August with a relatively larger Q than in September. The subpeak of the WC occurs during December to February when there is a large electricity demand for heating in the winter. However, the R during the winter is small due to the quite large Q . The cooling water consumption in October is comparable with that in January, but leaves much larger impacts on water resources due to the lower streamflow in October. The most serious impacts on water resources occur during August to October with the largest R when the

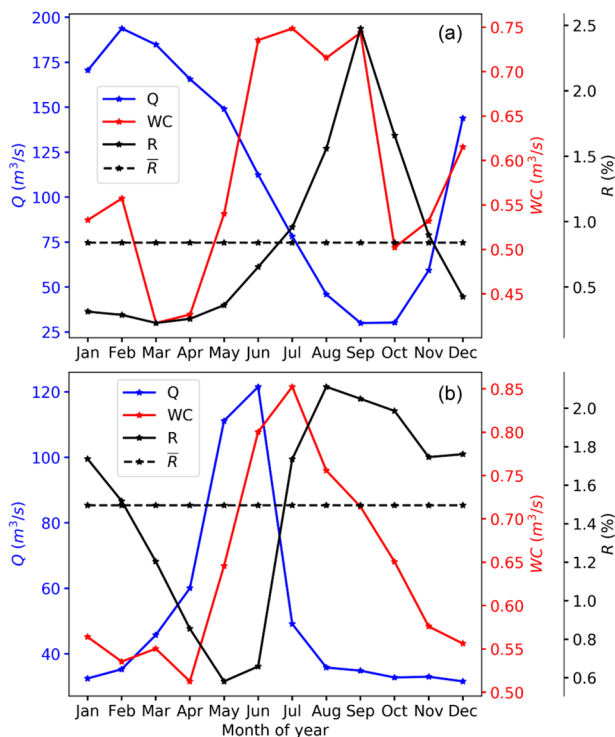


Figure 3. Mean monthly streamflow (Q), cooling water consumption (WC), the percentage (R) of WC to Q , and the average (\bar{R}) of the percentages in (a) Kaskaskia River watershed and (b) San Juan River watershed.

streamflow is low and power plants compete with other water users for limited water resources. The temporal patterns of the Q , WC , and R are quite different in the San Juan River watershed (Figure 3b). The peak streamflow occurs in June and the low streamflow lasts from August to February, or half of the year. The peak WC occurs in June to August. The largest R is in Aug when the WC is large and the Q is the smallest. The most serious impacts on water resources occur in August to October, which is the same as in the Kaskaskia River watershed. The long-term average percentage (\bar{R}) in San Juan is almost double that of Kaskaskia, indicating that in the long run and at an annual scale, the cooling water consumption in San Juan has a greater impact on streamflow. In dry seasons, however, the largest R in Kaskaskia is 25% larger than that in San Juan, which indicates that at the seasonal scale, the water–electricity nexus may be more vulnerable in Kaskaskia during dry periods.

The temporal variability of the R is much more significant at the daily scale than at the mean monthly scale. This is due to the fact that daily streamflow is much more variable than monthly streamflow in the two watersheds. In Figure 4, the R is quite large on some dry days with very small streamflow. However, at the mean monthly scale as in Figure 3, the small streamflow on dry days would be averaged with the large streamflow on wet days, leading to a small R . As shown in Figure 4a, in Kaskaskia, the daily R can be as high as 30% during the 1988 drought on account of the lowest streamflow of the year and the large cooling water demand. During the low flow or drought periods, other water consumers usually also have a large demand for the limited water resources. Therefore, the potential water–electricity trade-offs and electricity supply risk would emerge if a water consumption policy constraint

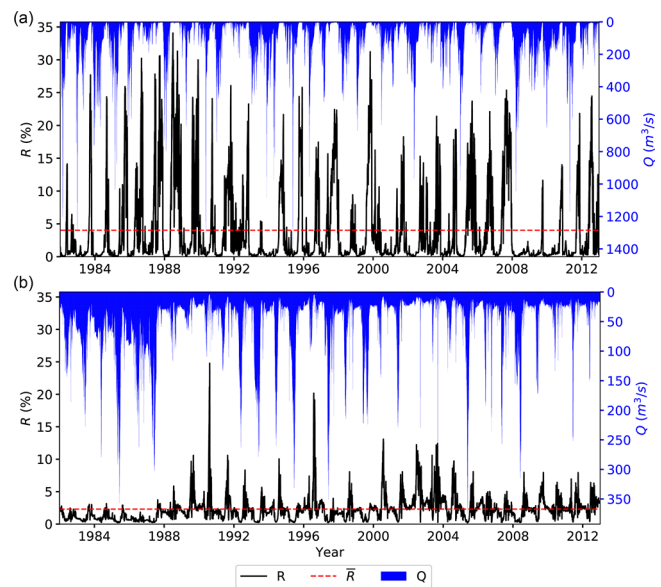


Figure 4. Daily cooling water consumption percentage (R) during 1982–2012, the average (\bar{R}) of daily percentages, and streamflow (Q) in (a) Kaskaskia River watershed, (b) San Juan River watershed.

were adopted to limit the R . In San Juan (Figure 4b), the largest R is around 20% which is much smaller than that in Kaskaskia, mainly because of its relatively large streamflow in low flow seasons, although its annual streamflow ($52 \text{ m}^3/\text{s}$) is only 46% of that in Kaskaskia ($113 \text{ m}^3/\text{s}$). In the long run, the average daily percentage (\bar{R}) (red dashed line) in San Juan (2.3%) is 58% of that in Kaskaskia (4%), which is quite contrary to the results at the long-term mean monthly scale in Figure 3. This indicates the importance of considering daily variabilities of water resources and cooling water consumption in the risk assessment as we do in this study.

3.2. Seasonal Risk of Water–Electricity Nexus under Water Consumption Policy Constraint. This section demonstrates the seasonal risk of the water–electricity nexus under the water consumption policy constraint in terms of the allowed maximum cooling water consumption percentage (R^0). Instead of using calendar seasons, we choose the three most vulnerable months with the maximum R as the August–September–October (ASO) season based on Figure 3 in Section 3.1. The other three seasons are determined chronologically: November–December–January (NDJ), February–March–April (FMA), and May–June–July (MJJ). The three indicators defined in Section 2.3 are plotted for the whole period (denoted by “Year”) and each season (denoted by “ASO”, “NDJ”, “FMA”, “MJJ”) in two representative watersheds. In each panel of the Figure 5, the x -axis starts from the long-term average \bar{R} (red dashed line in Figure 4) of the daily cooling water consumption percentages and ends with the maximum required percentage (the peak value of R in Figure 4) that guarantees sufficient cooling water availability on every single day to support electricity generation.

In Figure 5a and 5d, the reliability (Rel) of maintaining a historic level of electricity generation under the varying allowed maximum cooling water consumption percentages (R^0) is shown. In Kaskaskia (Figure 5a), when R^0 is set as the long-term average percentage \bar{R} (4%), the Rel is around 40% during the ASO season so that only 40% of the days during ASO can be supplied with the desired electricity demand when

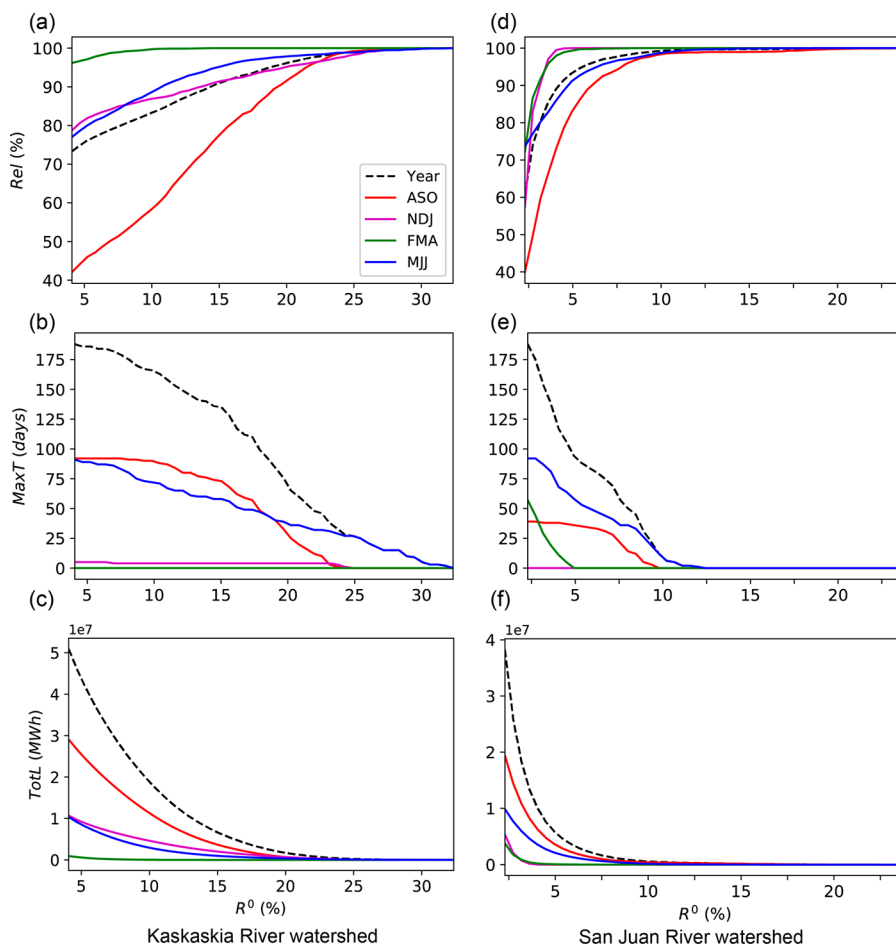


Figure 5. Reliability (Rel), maximum time to recovery (MaxT), and total power generation loss (TotL) in the whole period (“Year”) and four seasons (“ASO”, “NDJ”, “FMA”, “MJJ”) during 1982–2012 based on variable cooling water consumption intensities in (a), (b), (c) Kaskaskia River watershed and (d), (e), (f) San Juan River watershed under different water consumption policy constraints in terms of the allowed maximum cooling water consumption percentage (R^0).

cooling water availability is constrained. The Rel is around 80% in NDJ and MJJ and is larger than 95% in FMA on account of the large streamflow, indicating a high reliability during these three seasons, even under a strict water consumption policy constraint. When R^0 increases and the water consumption policy constraint is relaxed, the Rel increases in all seasons, with the most rapid increase in the typically dry season ASO. The R^0 needs to be increased to 25% if a nearly 100% reliability is desired in all seasons, which indicates that 25% of the water resources would be consumed during some dry days by this single power plant, leaving less water for other water users. In San Juan (Figure 5d), when R^0 is set at the level of the \bar{R} (2.3%), the Rel is around 40% during ASO, which is comparable to that in Kaskaskia. However, the Rel is 60–75% during the other three seasons, which is much smaller than that in Kaskaskia. The Rel increases with the R^0 more rapidly in San Juan than in Kaskaskia. A nearly 100% reliability can be guaranteed when the R^0 is 12.5%, which is only half of that in Kaskaskia and represents less impact of the consumptive cooling water use on water resources.

Figure 5b and 5e show the maximum time to recovery (MaxT) from an electricity undersupply period. The value of MaxT at the “Year” scale shown by black dashed line is the sum of MaxT in the four seasons. In Kaskaskia (Figure 5b), when R^0 is set as \bar{R} (4%), the MaxT is 92 days in ASO and MJJ, which means that the undersupply cases would occur

throughout these two seasons in the year 1988 (see SI Figure S3). Compared with the Rel in Figure 5a, although MJJ has a relatively large Rel from the long-term perspective, the undersupply case may last throughout MJJ season during the extremely dry year. This shows the advantages of the MaxT indicator rather than using only a single indicator, that is, reliability, to identify a potential risky season. The MaxT shows a nonlinear relationship with the R^0 : MaxT is more (less) quickly decreased in MJJ than in ASO when R^0 is smaller (larger) than 18%, which implicates that the most serious water–electricity nexus trade-off in 1988 occurs in MJJ rather than in ASO (i.e., the smallest usable capacity in SI Figure S3 occurs in MJJ). The MaxT appears as a flat line, for example, in ASO season with R^0 less than 10%, because the increase of R^0 does not reach a critical point which could increase usable capacity beyond historic power output. In San Juan (Figure 5e), the largest MaxT occurs in MJJ season of the year 2002. Compared to Kaskaskia, the MaxT decreases more quickly in San Juan with R^0 . The MaxT in all seasons in San Juan would be reduced to a low level when the R^0 is increased to 10%, while in Kaskaskia, the R^0 needs to be increased around 30% to maintain a similar low level of the MaxT.

Figure 5c and 5f show the total power generation loss (TotL) during electricity undersupply periods. In Kaskaskia (Figure 5c), when R^0 is set as the \bar{R} (4%), TotL is around 5×10^7 MWh during 1982–2012, with 60% of the loss, that is, $3 \times$

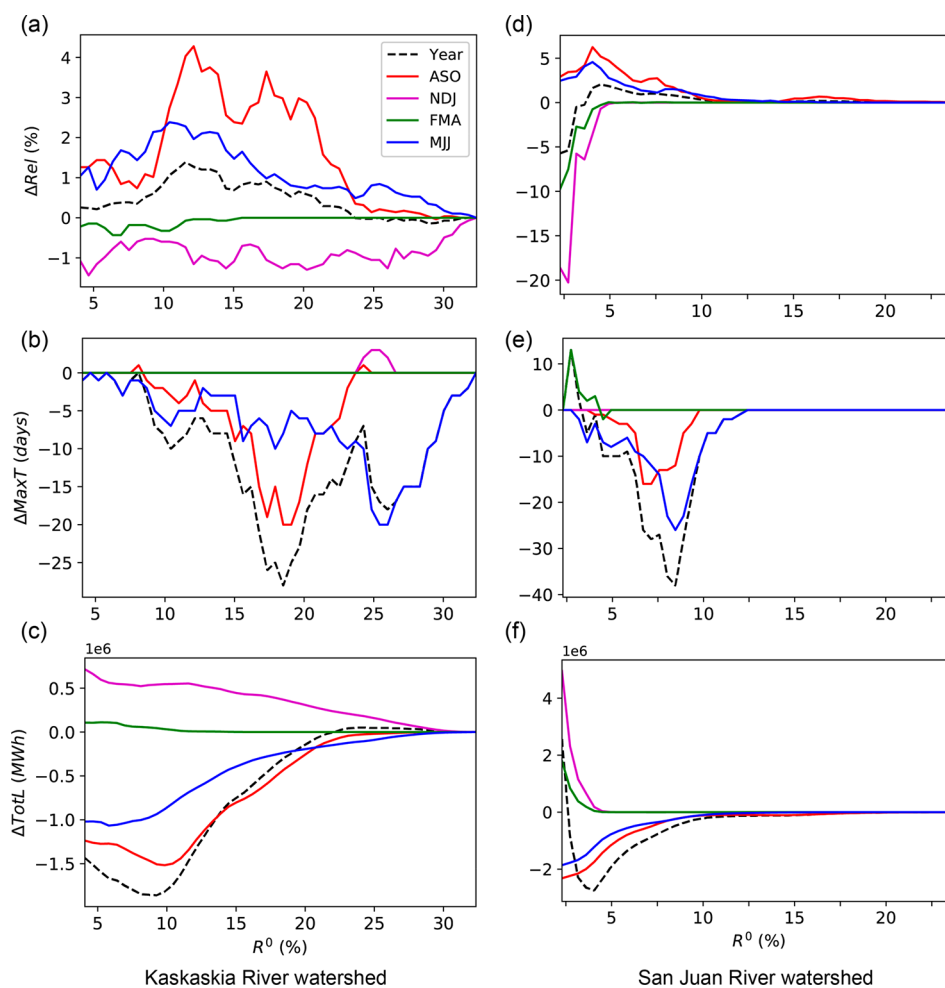


Figure 6. Differences in reliability (Rel), maximum time to recovery (MaxT), and total power generation loss (TotL) in the whole year and four seasons during 1982–2012 based on a constant average and variable cooling water consumption intensities in (a), (b), (c) Kaskaskia River watershed and (d), (e), (f) San Juan River watershed under different water consumption policy constraints in terms of the allowed maximum cooling water consumption percentage (R^0).

10^7 MWh, in ASO season. Around 20% of the loss occurs in both NDJ and MJJ seasons, while the loss in FMA season is minimal. The TotL is decreased with R^0 , more rapidly in ASO season. In San Juan (Figure 5f), when R^0 is set as the \bar{R} (2.3%), TotL is around 4×10^7 MWh during 1982–2012, with 50% of the loss, that is, 2×10^7 MWh, in ASO season.

When a same R^0 is adopted in the two watersheds, the risk is much smaller, (represented by a larger Rel, smaller MaxT and TotL in Figure 5), in all seasons in San Juan than that in Kaskaskia, although San Juan has only half of the annual streamflow that Kaskaskia has in the long-run perspective. For example, when R^0 is set as 10%, the Rel is around 60% in ASO and 90% in NDJ and MJJ in Kaskaskia, and the Rel in San Juan is higher than 95% in all seasons. The seasonal differences of the Rel are much larger in Kaskaskia on account of the relatively large seasonal variability in streamflow. Under the same water consumption policy constraint (R^0), the water–electricity nexus is generally more reliable in San Juan than in Kaskaskia in all seasons. The nexus risk would be significantly underestimated in dry seasons (i.e., ASO) when the risk assessment is conducted throughout the whole period (shown by the black dashed line in Figure 5) rather than at the seasonal scale, which indicates the importance of the seasonal-scale assessment.

3.3. The Necessity of Considering Variable Cooling Water Consumption Intensities. To illustrate the advantages of using the variable cooling water consumption intensities (WIs) in the current seasonal risk assessment, we calculate the three indicators based on a constant long-term average WI and compare them with the results shown in Figure 5 in Section 3.2. As shown in Figure 6, the water–electricity nexus risk would generally be underestimated (represented by the positive ΔRel , negative $\Delta MaxT$ and $\Delta TotL$) during dry seasons (ASO and MJJ) and overestimated during wet seasons (NDJ and FMA) both in the Kaskaskia and San Juan River watersheds, caused by the underestimated and overestimated WI in dry and wet seasons, respectively. Therefore, variable cooling water consumption intensities need to be considered to avoid over or underestimating the three indicators and the associated water–electricity nexus risk.

4. DISCUSSION

In this study, the seasonal risk of the water–electricity nexus in two representative watersheds is revealed using the proposed risk assessment method. The results demonstrate that the nexus risk is highly seasonal and is greatly impacted by the seasonal streamflow variability rather than the magnitude of the annual or long-term mean streamflow. Under the same

water consumption policy constraint, the nexus is found to be more risky (represented by smaller Rel, larger MaxT and TotL) in the Kaskaskia River watershed with its larger mean annual streamflow and larger seasonal variability than in the San Juan River watershed with a smaller mean annual streamflow and smaller variability. The reason for this result is that the streamflow (Figures 3 and 4) during dry seasons is relatively large in San Juan, although the long-term average streamflow is only 46% of that in Kaskaskia. This study highlights the advantages of a seasonal-scale risk assessment method over an annual or long-term scale technique. Overlooking the seasonality of the available water resources and cooling water consumption may lead to biased conclusions when identifying the risky watersheds and seasons. In addition, using variable cooling water consumption intensities over various periods rather than a constant long-term average is found necessary to avoid underestimating the risk during dry seasons (ASO and MJJ) and overestimating during wet seasons (NDJ and FMA) (Figure 6).

This study provides implications to water consumption policymakers such as the Department of Natural Resources and the River Basin Commission. Although an integrated index may be easier to practice, it would mask the different dimensions of the nexus trade-offs which are revealed by the three indicators with more policy implications. Based on the three risk indicators, properly adopting an allowed maximum cooling water consumption percentage (R^0) is critical to balancing the trade-off between surface water resources reservation and electricity generation. A policy based on the long-term average R^0 would usually significantly constrain the cooling water availability and thus electricity generation during low flow or dry seasons, especially in an extremely dry year, such as 1988 and 2012 in the Kaskaskia River watershed. The daily percentage (R^0) is used to demonstrate the limitation of the yearly percentage used in previous studies, which is not adequate, though more administratively practical, to show the interimpacts of water and energy systems. The purpose of this study is to reveal the daily to seasonal risk and try to provide some implications for policy makers to set effective water consumption policies at a fine temporal scale, for example, at the monthly scale rather than annual scale. However, many factors, for example, the cost and difficulty to implement the policy and its feasibility, need to be considered to make a final policy decision, which is beyond the scope of our current study. Under a strict constraint, power plants may exploit other water sources such as groundwater and reusable wastewater to maintain a high level of electricity supply, which would increase the operating cost⁵¹ or cause some unintended consequences to the water system. Relaxing the water consumption policy constraint by increasing the R^0 is necessary in dry seasons to guarantee adequate cooling water availability but would also affect other water consumers in the same watershed. In this study, we assume that there are no water storage facilities at the plant to regulate or mitigate the natural streamflow variability. Such facilities can store water in wet seasons and provide sufficient cooling water in dry seasons, thereby reducing the risk of the water–electricity nexus but with a large capital investment. Attention should also be paid to the potential large risk during typically wet seasons in a dry year, although in the long run, the nexus is generally reliable in wet seasons.

This study analyzes the seasonal risk of the electricity supply at a power plant level. However, a power grid is usually

composed of a significant number of plants and extends over a large region rather than a small watershed. The water–electricity nexus risk at some plants may be offset by other plants that have sufficient cooling water availability in the same grid but can also be aggravated if the watersheds are simultaneously hit by low flow and drought events. Future works involve extending the proposed risk assessment method from the power plant level to the power grid level to advance our understanding of the water–electricity nexus risk from a system perspective.

■ ASSOCIATED CONTENT

SI Supporting Information

The Supporting Information is available free of charge at <https://pubs.acs.org/doi/10.1021/acs.est.0c00171>.

Text, tables, and figures regarding input data sources, study areas, the fundamentals of cooling water consumption estimation module in IECM, sensitivity test of cooling water consumption intensity to air temperature and relative humidity, seasonality of cooling water consumption intensity, constrained usable capacity under water consumption policy constraint, constrained cooling water consumption under water consumption policy constraint(PDF)

■ AUTHOR INFORMATION

Corresponding Authors

Zhenxing Zhang – Illinois State Water Survey, Prairie Research Institute, University of Illinois at Urbana–Champaign, Champaign, Illinois 61820, United States; Email: zhang538@illinois.edu

Qihong Tang – Key Laboratory of Water Cycle and Related Land Surface Processes, Institute of Geographical Sciences and Natural Resources Research, Chinese Academy of Sciences, Beijing 100101, China; University of Chinese Academy of Sciences, Beijing 100101, China; orcid.org/0000-0002-0886-6699; Email: tangqh@igsnrr.ac.cn

Authors

Mengfei Mu – Key Laboratory of Water Cycle and Related Land Surface Processes, Institute of Geographical Sciences and Natural Resources Research, Chinese Academy of Sciences, Beijing 100101, China; University of Chinese Academy of Sciences, Beijing 100101, China; Illinois State Water Survey, Prairie Research Institute, University of Illinois at Urbana–Champaign, Champaign, Illinois 61820, United States

Ximing Cai – Department of Civil and Environmental Engineering, University of Illinois at Urbana–Champaign, Urbana, Illinois 61801, United States

Complete contact information is available at: <https://pubs.acs.org/doi/10.1021/acs.est.0c00171>

Notes

The authors declare no competing financial interest.

■ ACKNOWLEDGMENTS

This work was supported by the National Natural Science Foundation of China (41790424, 41730645, 41425002), the Strategic Priority Research Program of Chinese Academy of Sciences (XDA20060402), and the International Partnership Program of Chinese Academy of Sciences

(131A11KYSB20180034). We are grateful to Lisa Sheppard for the editorial review.

REFERENCES

- (1) Spang, E. S.; Moomaw, W. R.; Gallagher, K. S.; Kirshen, P. H.; Marks, D. H. The Water Consumption of Energy Production: An International Comparison. *Environ. Res. Lett.* **2014**, *9* (10), 105002.
- (2) Macknick, J.; Sattler, S.; Averyt, K.; Clemmer, S.; Rogers, J. The Water Implications of Generating Electricity: Water Use across the United States Based on Different Electricity Pathways through 2050. *Environ. Res. Lett.* **2012**, *7* (4), 045803.
- (3) Averyt, K.; Macknick, J.; Rogers, J.; Madden, N.; Fisher, J.; Meldrum, J.; Newmark, R. Water Use for Electricity in the United States: An Analysis of Reported and Calculated Water Use Information for 2008. *Environ. Res. Lett.* **2013**, *8* (1), 015001.
- (4) Daher, B. T.; Mohtar, R. H. Water–Energy–Food (WEF) Nexus Tool 2.0: Guiding Integrative Resource Planning and Decision-Making. *Water Int.* **2015**, *40* (5–6), 748–771.
- (5) Daher, B.; Hannibal, B.; Portney, K. E.; Mohtar, R. H. Toward Creating an Environment of Cooperation between Water, Energy, and Food Stakeholders in San Antonio. *Sci. Total Environ.* **2019**, *651*, 2913–2926.
- (6) Qin, Y.; Curmi, E.; Kopec, G. M.; Allwood, J. M.; Richards, K. S. China's Energy-Water Nexus - Assessment of the Energy Sector's Compliance with the "3 Red Lines" Industrial Water Policy. *Energy Policy* **2015**, *82* (1), 131–143.
- (7) Liao, X.; Hall, J. W.; Eyre, N. Water Use in China's Thermoelectric Power Sector. *Glob. Environ. Change* **2016**, *41*, 142–152.
- (8) Zhang, X.; Liu, J.; Tang, Y.; Zhao, X.; Yang, H.; Gerbens-Leenes, P. W.; van Vliet, M. T. H.; Yan, J. China's Coal-Fired Power Plants Impose Pressure on Water Resources. *J. Cleaner Prod.* **2017**, *161*, 1171–1179.
- (9) Byers, E. A.; Hall, J. W.; Amezaga, J. M. Electricity Generation and Cooling Water Use: UK Pathways to 2050. *Glob. Environ. Change* **2014**, *25* (1), 16–30.
- (10) Davies, E. G. R.; Kyle, P.; Edmonds, J. A. An Integrated Assessment of Global and Regional Water Demands for Electricity Generation to 2095. *Adv. Water Resour.* **2013**, *52*, 296–313.
- (11) van Vliet, M. T. H.; Yearsley, J. R.; Ludwig, F.; Vögele, S.; Lettenmaier, D. P.; Kabat, P. Vulnerability of US and European Electricity Supply to Climate Change. *Nat. Clim. Change* **2012**, *2* (9), 676–681.
- (12) van Vliet, M. T. H.; Wiberg, D.; Leduc, S.; Riahi, K. Power-Generation System Vulnerability and Adaptation to Changes in Climate and Water Resources. *Nat. Clim. Change* **2016**, *6* (4), 375.
- (13) Zhou, Q.; Hanasaki, N.; Fujimori, S.; Yoshikawa, S.; Kanae, S.; Okadera, T. Cooling Water Sufficiency in a Warming World: Projection Using an Integrated Assessment Model and a Global Hydrological Model. *Water* **2018**, *10* (7), 872.
- (14) Sesma-Martín, D. The River's Light: Water Needs for Thermoelectric Power Generation in the Ebro River Basin, 1969–2015. *Water* **2019**, *11* (3), 441.
- (15) Averyt, K.; Meldrum, J.; Caldwell, P.; Sun, G.; McNulty, S.; Huber-Lee, A.; Madden, N. Sectoral Contributions to Surface Water Stress in the Conterminous United States. *Environ. Res. Lett.* **2013**, *8* (3), 035046.
- (16) Diehl, T. H.; Harris, M. A. Withdrawal and Consumption of Water by Thermoelectric Power Plants in the United States, 2010: *Sci. Invest. Rep.*; **2014**. DOI: 10.3133/sir20145184.
- (17) Tidwell, V. C.; Bailey, M.; Zemlick, K. M.; Moreland, B. D. Water Supply as a Constraint on Transmission Expansion Planning in the Western Interconnection. *Environ. Res. Lett.* **2016**, *11* (12), 124001.
- (18) Liu, L.; Hejazi, M.; Patel, P.; Kyle, P.; Davies, E.; Zhou, Y.; Clarke, L.; Edmonds, J. Water Demands for Electricity Generation in the U.S.: Modeling Different Scenarios for the Water–Energy Nexus. *Technol. Forecast. Soc. Change* **2015**, *94*, 318–334.
- (19) Liu, L.; Hejazi, M.; Iyer, G.; Forman, B. A. Implications of Water Constraints on Electricity Capacity Expansion in the United States. *Nat. Sustain.* **2019**, *2* (3), 206.
- (20) Jiang, D.; Ramaswami, A. The 'thirsty' Water-Electricity Nexus: Field Data on the Scale and Seasonality of Thermoelectric Power Generation's Water Intensity in China. *Environ. Res. Lett.* **2015**, *10* (2), 024015.
- (21) Gaudard, L.; Avanzi, F.; De Michele, C. Seasonal Aspects of the Energy-Water Nexus: The Case of a Run-of-the-River Hydropower Plant. *Appl. Energy* **2018**, *210*, 604–612.
- (22) Qin, Y.; Mueller, N. D.; Siebert, S.; Jackson, R. B.; AghaKouchak, A.; Zimmerman, J. B.; Tong, D.; Hong, C.; Davis, S. J. Flexibility and Intensity of Global Water Use. *Nat. Sustain.* **2019**, *2* (6), 515.
- (23) Lubega, W. N.; Stillwell, A. S. Maintaining Electric Grid Reliability under Hydrologic Drought and Heat Wave Conditions. *Appl. Energy* **2018**, *210*, 538–549.
- (24) Gleick, P. H. Water and Energy. *Annu. Rev. Energy Environ.* **1994**, *19* (1), 267–299.
- (25) Macknick, J.; Newmark, R.; Heath, G.; Hallett, K. C. Operational Water Consumption and Withdrawal Factors for Electricity Generating Technologies: A Review of Existing Literature. *Environ. Res. Lett.* **2012**, *7* (4), 045802.
- (26) Meldrum, J.; Nettles-Anderson, S.; Heath, G.; Macknick, J. Life Cycle Water Use for Electricity Generation: A Review and Harmonization of Literature Estimates. *Environ. Res. Lett.* **2013**, *8* (1), 015031.
- (27) NETL. Cost and Performance Baseline for Fossil Energy Plants Vol. 1a: Bituminous Coal (PC) and Natural Gas to Electricity Revision 3. In *Carbon Capture Reports*, DOE/NETL-2015/1723; National Energy Technology Laboratory, 2015.
- (28) Berkenpas, M. P.; Kietzke, K.; Mantripragada, H.; McCoy, S. T.; Rubin, E. S.; Versteeg, P. L.; Zhai, H. *IECM Technical Documentation Updates Final Report*. **2009**, 1–5.
- (29) Zhai, H.; Rubin, E. S.; Versteeg, P. L. Water Use at Pulverized Coal Power Plants with Postcombustion Carbon Capture and Storage. *Environ. Sci. Technol.* **2011**, *45* (6), 2479–2485.
- (30) Berkenpas, M. B.; Fry, J. J.; Kietzke, K.; Rubin, E. S. *IECM User Documentation: User Manual*. **2018**.
- (31) Talati, S.; Zhai, H.; Kyle, G. P.; Morgan, M. G.; Patel, P.; Liu, L. Consumptive Water Use from Electricity Generation in the Southwest under Alternative Climate, Technology, and Policy Futures. *Environ. Sci. Technol.* **2016**, *50* (22), 12095–12104.
- (32) Gjorgiev, B.; Sansavini, G. Electrical Power Generation under Policy Constrained Water-Energy Nexus. *Appl. Energy* **2018**, *210*, 568–579.
- (33) Mu, M.; Zhang, Z.; Cai, X.; Tang, Q. A Water-Electricity Nexus Model to Analyze Thermoelectricity Supply Reliability under Environmental Regulations and Economic Penalties during Drought Events. *Environ. Model. Softw.* **2020**, *123*, 104514.
- (34) Hashimoto, T.; Stedinger, J. R.; Loucks, D. P. Reliability, Resiliency, and Vulnerability Criteria for Water Resource System Performance Evaluation. *Water Resour. Res.* **1982**, *18* (1), 14–20.
- (35) Loucks, D. P.; Beek, E. van. *Water Resource Systems Planning and Management: An Introduction to Methods, Models, and Applications*; Springer International Publishing, 2017.
- (36) USGS. National Water Information System <http://waterdata.usgs.gov/nwis> (2018-5-1).
- (37) SRBC. Low Flow Protection Policy Related To Withdrawal Approvals <https://www.srb.net/regulatory/policies-guidance/> (accessed 2019-5-13).
- (38) Xia, Y.; Mitchell, K.; Ek, M.; Cosgrove, B.; Sheffield, J.; Luo, L.; Alonge, C.; Wei, H.; Meng, J.; Livneh, B.; Duan, Q.; Lohmann, D. Continental-Scale Water and Energy Flux Analysis and Validation for North American Land Data Assimilation System Project Phase 2 (NLDAS-2): 2. Validation of Model-Simulated Streamflow. *J. Geophys. Res., Atmos.* **2012**, *117* (D3).
- (39) Xia, Y.; Mitchell, K.; Ek, M.; Sheffield, J.; Cosgrove, B.; Wood, E.; Luo, L.; Alonge, C.; Wei, H.; Meng, J.; Livneh, B.; Lettenmaier, D.,

Koren, V.; Duan, Q.; Mo, K.; Fan, Y.; Mocko, D. Continental-Scale Water and Energy Flux Analysis and Validation for the North American Land Data Assimilation System Project Phase 2 (NLDAS-2): 1. Intercomparison and Application of Model Products. *J. Geophys. Res., Atmos.* **2012**, *117* (D3).

(40) EIA. Form EIA-860 Detailed Data <https://www.eia.gov/electricity/data/eia860/> (accessed 2018-4-18).

(41) Talati, S.; Zhai, H.; Morgan, M. G. Water Impacts of CO₂ Emission Performance Standards for Fossil Fuel-Fired Power Plants. *Environ. Sci. Technol.* **2014**, *48* (20), 11769–11776.

(42) Zhai, H.; Rubin, E. S. Water Impacts of a Low-Carbon Electric Power Future: Assessment Methodology and Status. *Curr. Sustain. Energy Rep.* **2015**, *2* (1), 1–9.

(43) Ou, Y.; Zhai, H.; Rubin, E. S. Life Cycle Water Use of Coal- and Natural-Gas-Fired Power Plants with and without Carbon Capture and Storage. *Int. J. Greenhouse Gas Control* **2016**, *44*, 249–261.

(44) Portmann, R. W.; Solomon, S.; Hegerl, G. C. Spatial and Seasonal Patterns in Climate Change, Temperatures, and Precipitation across the United States. *Proc. Natl. Acad. Sci. U. S. A.* **2009**, *106* (18), 7324–7329.

(45) Bartos, M. D.; Chester, M. V. Impacts of Climate Change on Electric Power Supply in the Western United States. *Nat. Clim. Change* **2015**, *5* (8), 748–752.

(46) Peixoto, J. P.; Oort, A. H. The Climatology of Relative Humidity in the Atmosphere. *J. Clim.* **1996**, *9* (12), 3443–3463.

(47) Lawrence, M. G. The Relationship between Relative Humidity and the Dewpoint Temperature in Moist Air: A Simple Conversion and Applications. *Bull. Am. Meteorol. Soc.* **2005**, *86* (2), 225–234.

(48) Moy, W.-S.; Cohon, J. L.; ReVelle, C. S. A Programming Model for Analysis of the Reliability, Resilience, and Vulnerability of a Water Supply Reservoir. *Water Resour. Res.* **1986**, *22* (4), 489–498.

(49) Sandoval-Solis, S.; McKinney, D. C.; Loucks, D. P. Sustainability Index for Water Resources Planning and Management. *J. Water Resour. Plan. Manag.* **2011**, *137* (5), 381–390.

(50) Zhang, C.; Xu, B.; Li, Y.; Fu, G. Exploring the Relationships among Reliability, Resilience, and Vulnerability of Water Supply Using Many-Objective Analysis. *J. Water Resour. Plan. Manag.* **2017**, *143* (8), 04017044.

(51) Tidwell, V. C.; Macknick, J.; Zemlick, K.; Sanchez, J.; Woldeyesus, T. Transitioning to Zero Freshwater Withdrawal in the U.S. for Thermoelectric Generation. *Appl. Energy* **2014**, *131*, 508–516.